

Supplement of Atmos. Chem. Phys., 15, 9345–9360, 2015
<http://www.atmos-chem-phys.net/15/9345/2015/>
doi:10.5194/acp-15-9345-2015-supplement
© Author(s) 2015. CC Attribution 3.0 License.



Supplement of

Regional-scale transport of air pollutants: impacts of Southern California emissions on Phoenix ground-level ozone concentrations

J. Li et al.

Correspondence to: J. Li (jialun.li@asu.edu)

The copyright of individual parts of the supplement might differ from the CC-BY 3.0 licence.

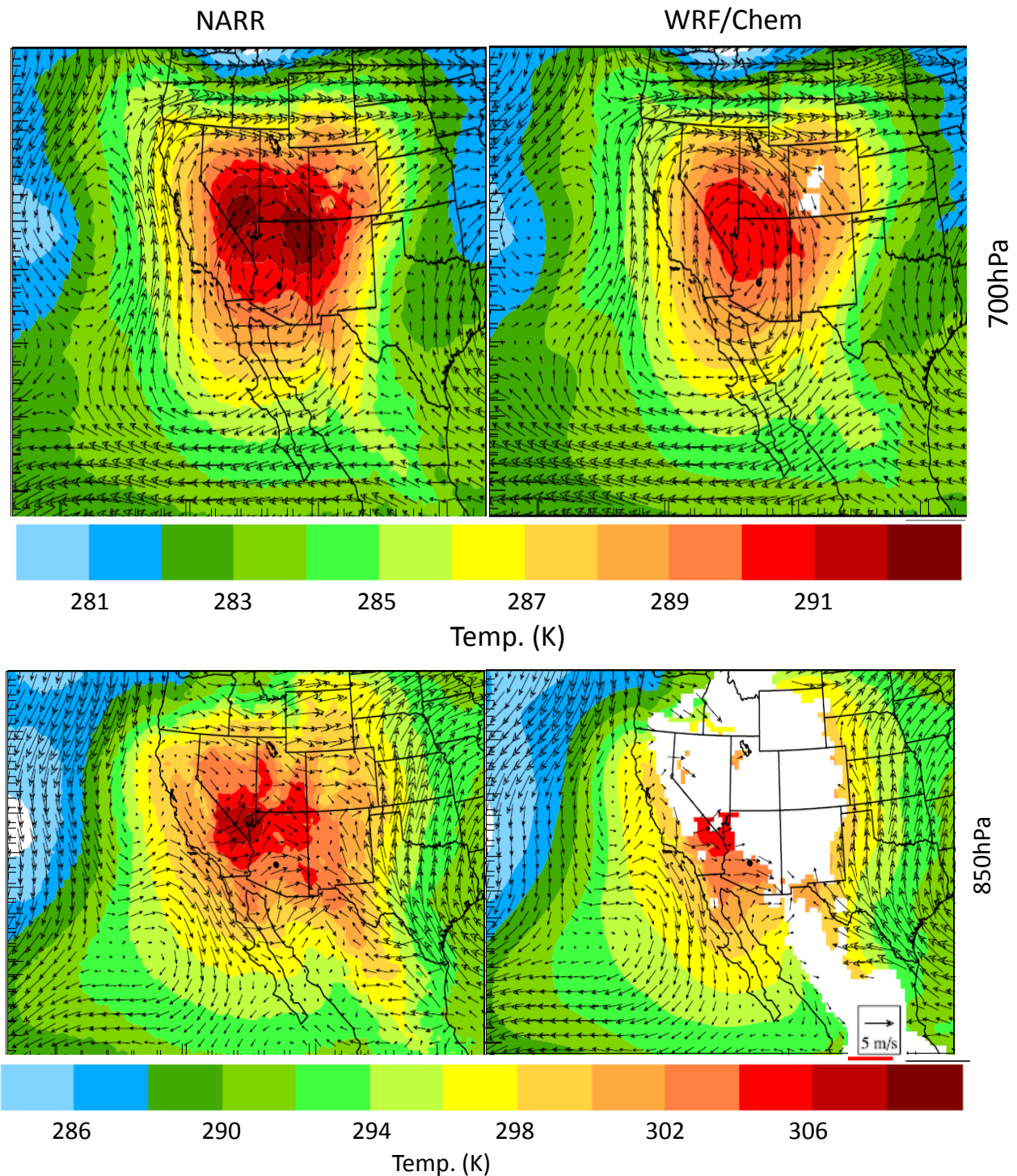


Figure S1: Averaged wind and temperature comparisons at 700 hPa and 850 hPa between WRF-Chem simulations and NARR data. The data are averaged from 16-19, July 2005. The masked areas in right column are the locations where terrain elevations are higher than the heights of 850 hPa (lower right) and 700 hPa (upper right). Generally, WRF-Chem simulations match the wind and temperature patterns of NARR data. In addition, at 850 hPa, there are westerly winds between southern California and Central Arizona in both sources.

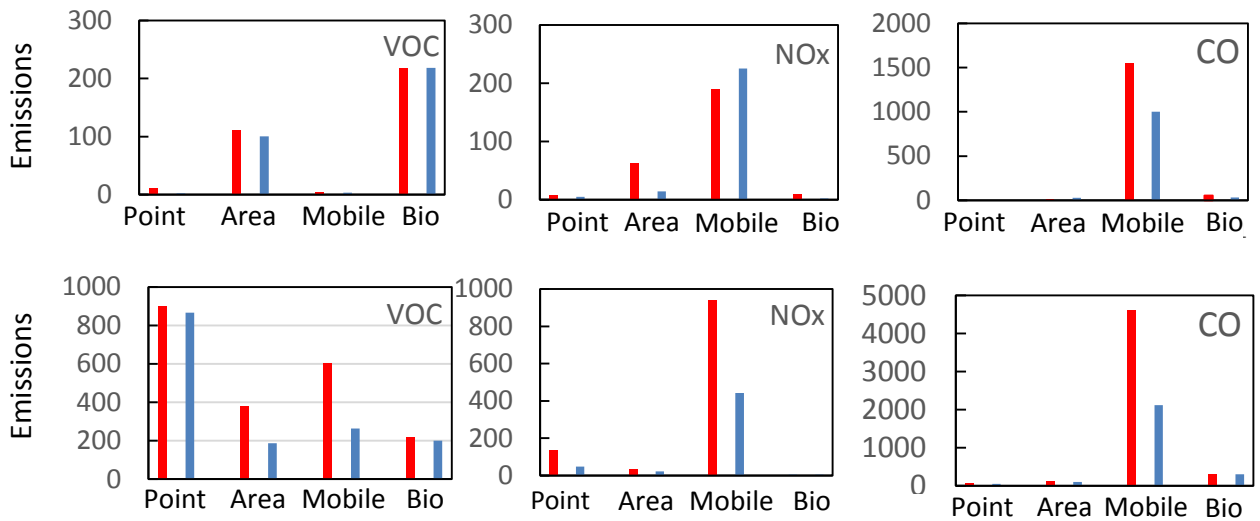


Figure S2: Emission (Ton per day) comparisons in Maricopa County (top panel), Arizona, and South Coast Airshed (bottom panel), California, between 2005 (red), and 2011(blue) for Maricopa County and 2012 for South Coast airshed. In South Coast Airshed, emissions from Mobile in 2012 are reduced significantly (40-50%), relative to 2005. The emission variations can explain the reasons of WRF-Chem overestimated the ozone precursors in May 2012 case. In Arizona, CO emissions from mobile are reduced. NOx emissions are reduced from Area but increased from Mobile.

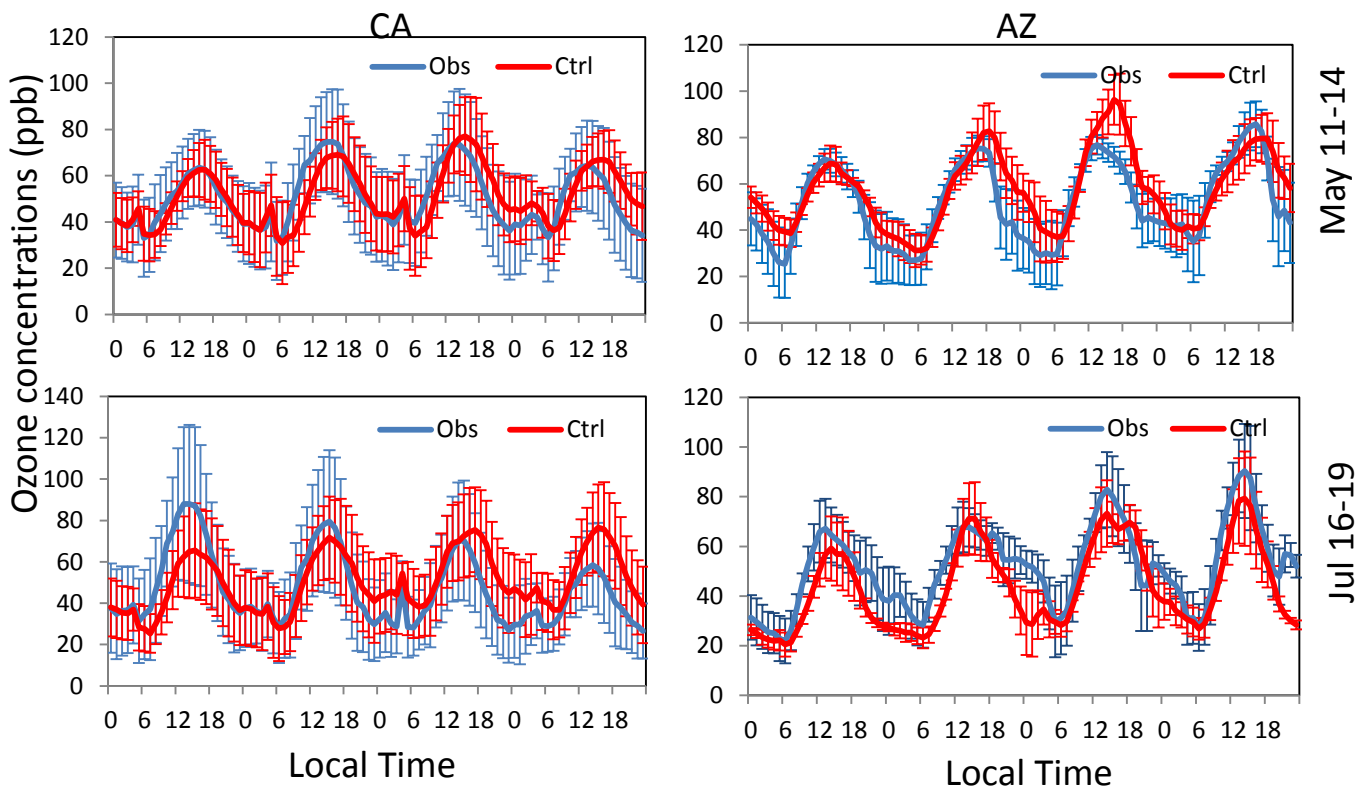


Figure S3: Ground-level ozone concentration comparisons between observations (blue) and simulations (red) in southern California and greater Phoenix, Arizona. The observation sites are labeled in Figure 1b (solid dots). There are about 46 sites for ozone observation in southern California and 24 sites in greater Phoenix. Ctrl represent WRF-Chem CTRL run.

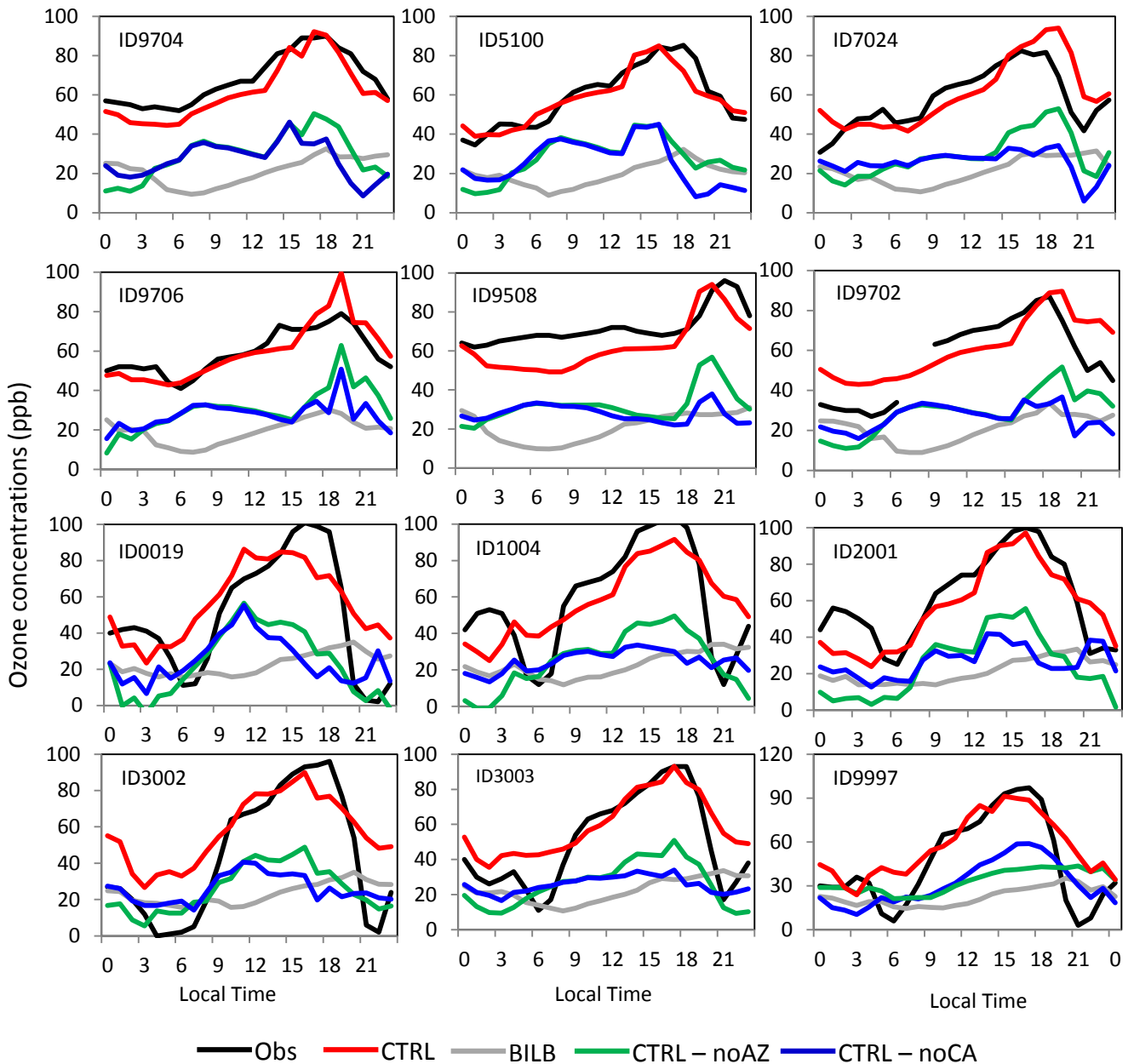


Figure S4: Relative contributions of different emission sources to ozone concentrations ($[O_3]$) at observation sites in Phoenix metropolitan area and surround rural. The date shown in the figure is May 14, 2012. IDxxxx indicates the site EPA AIRS number. The county number is 013, and state number is 04. In Figure, black line indicates the ozone observation. Red line represents the simulated ozone concentrations from CTRL run. Green line shows the $[O_3]$ differences between CTRL run and noAZ run. Blue line displays the ozone concentration differences between CTRL run and noCA run. Gray line is the ozone concentrations from BILB run.

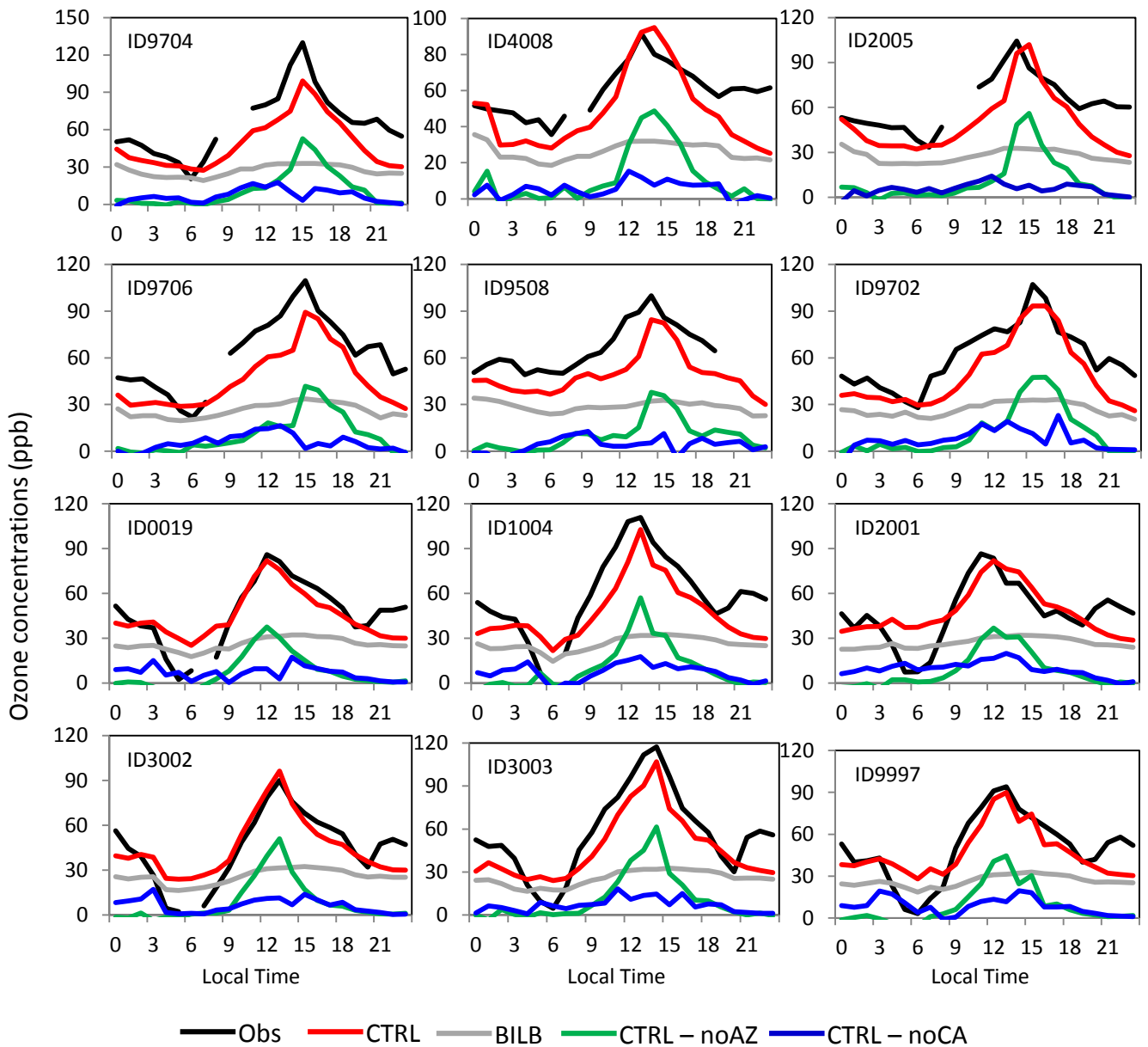


Figure S5: Relative contributions of different emissions sources to $[O_3]$ at observation sites in Phoenix metropolitan area and surround rural. The date shown in the figure is July 19, 2005. Idxxxx indicates the site EPA AIRS number. The county number is 013, and state number is 04. In Figure, black line indicates the ozone observation. Red line represents the simulated $[O_3]$ from CTRL run. Green line shows the ozone concentration differences between CTRL run and noAZ run. Blue line displays the ozone concentration differences between CTRL run and noCA run. Gray line is the ozone concentrations from BILB run.

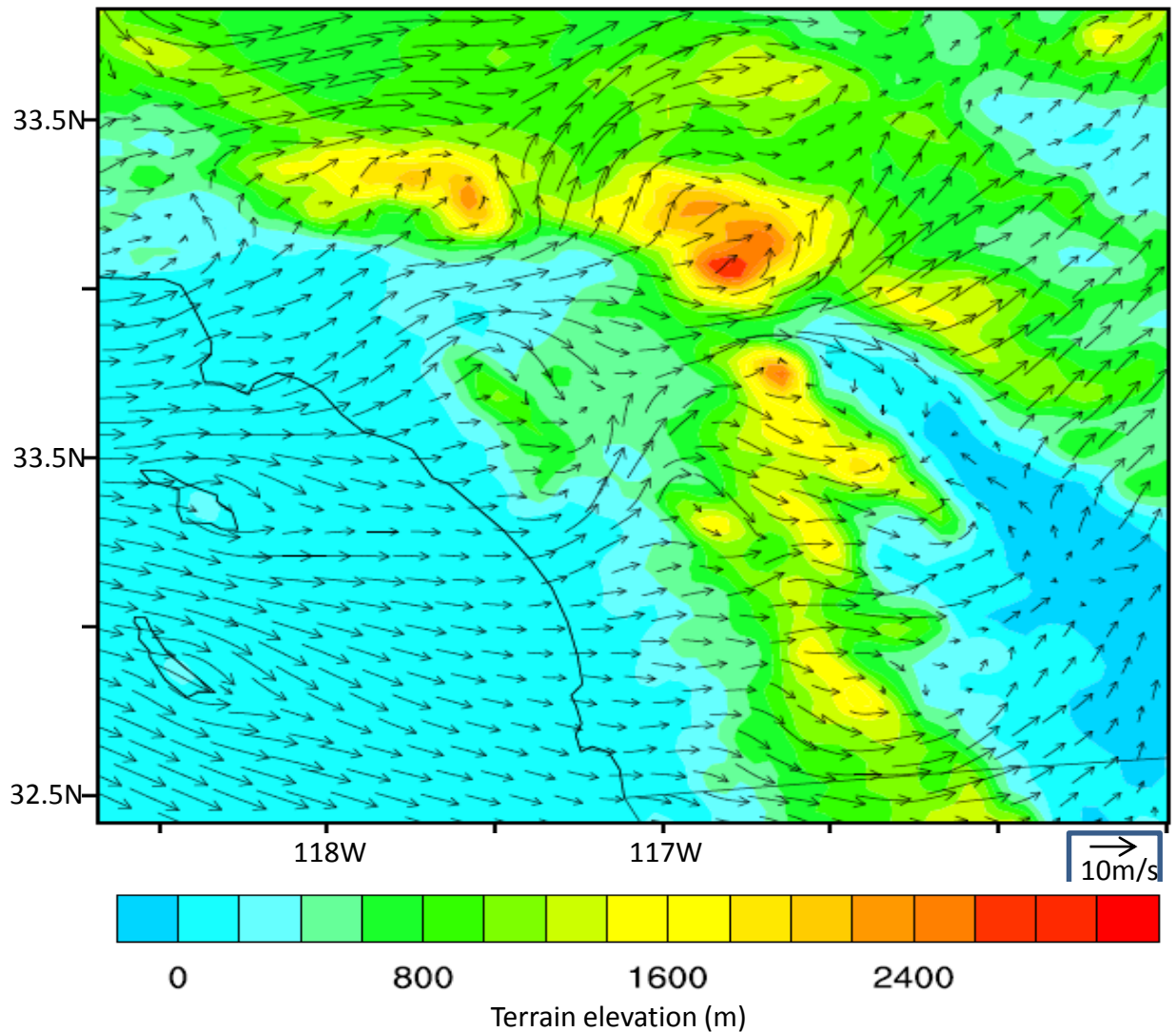


Figure S7: Day time mean of wind field vectors at 30 m a.g.l. from 4 km resolution run. Data are averaged over day time from July 16-20, 2005. There are the same patterns between Figure S7 and Figure 9 in general. However, there are differences in Salton Sea Airshed and Mojave Desert Airshed.

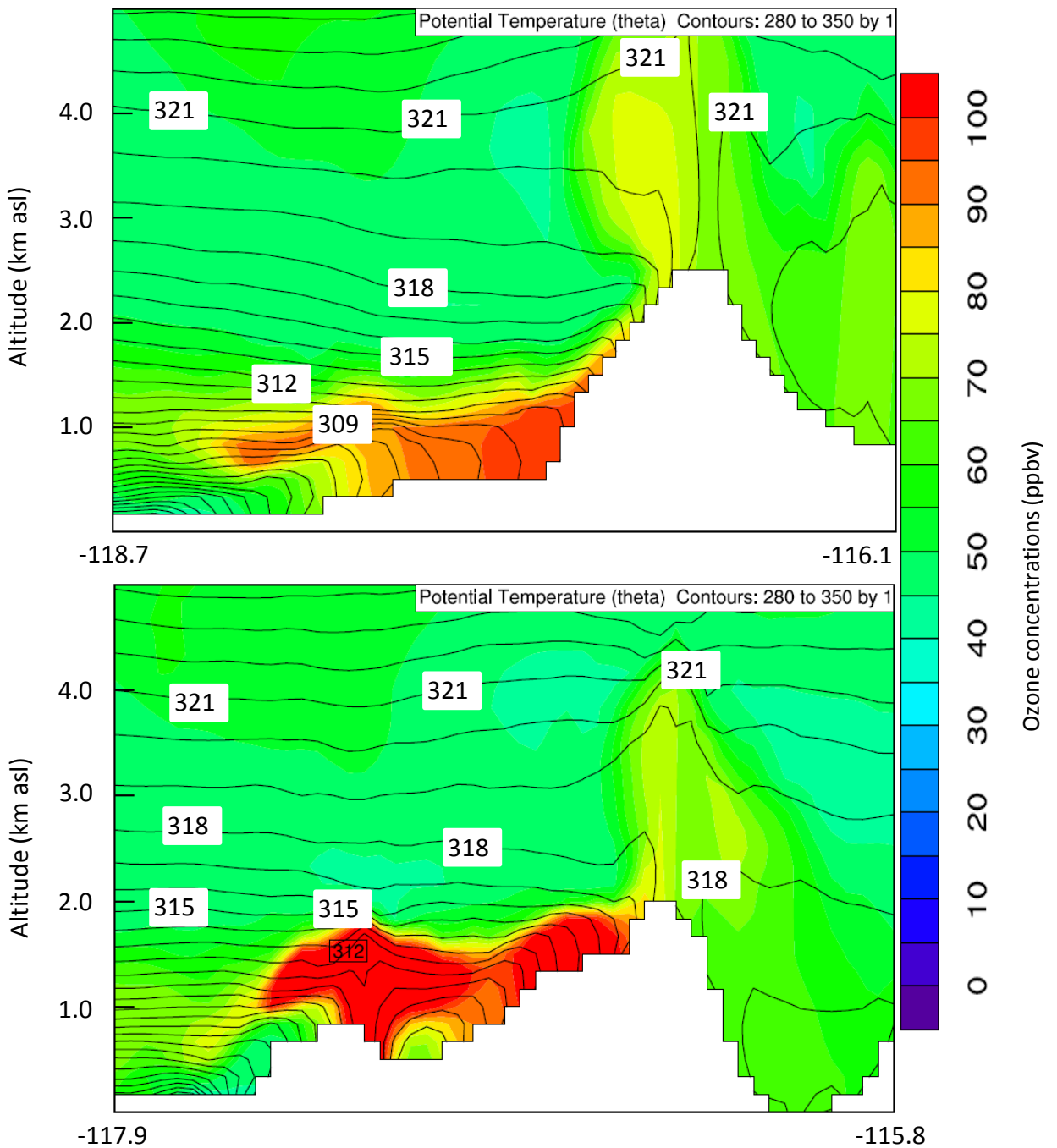


Figure S8: Vertical distributions of ozone along cross-section Lines A'A (top) and B'B (bottom) shown in Figure 1 at 22Z of July, 17, 2005. The contours are potential temperature starting at 280K with 1-K interval. Figures are plotted based on 4 km resolution run. Comparing Figure S8 with 1-km run (Figure 10 in manuscript), the Mountain Chimney Effect looks weaker at 4 km resolution than that at 1 km resolution.

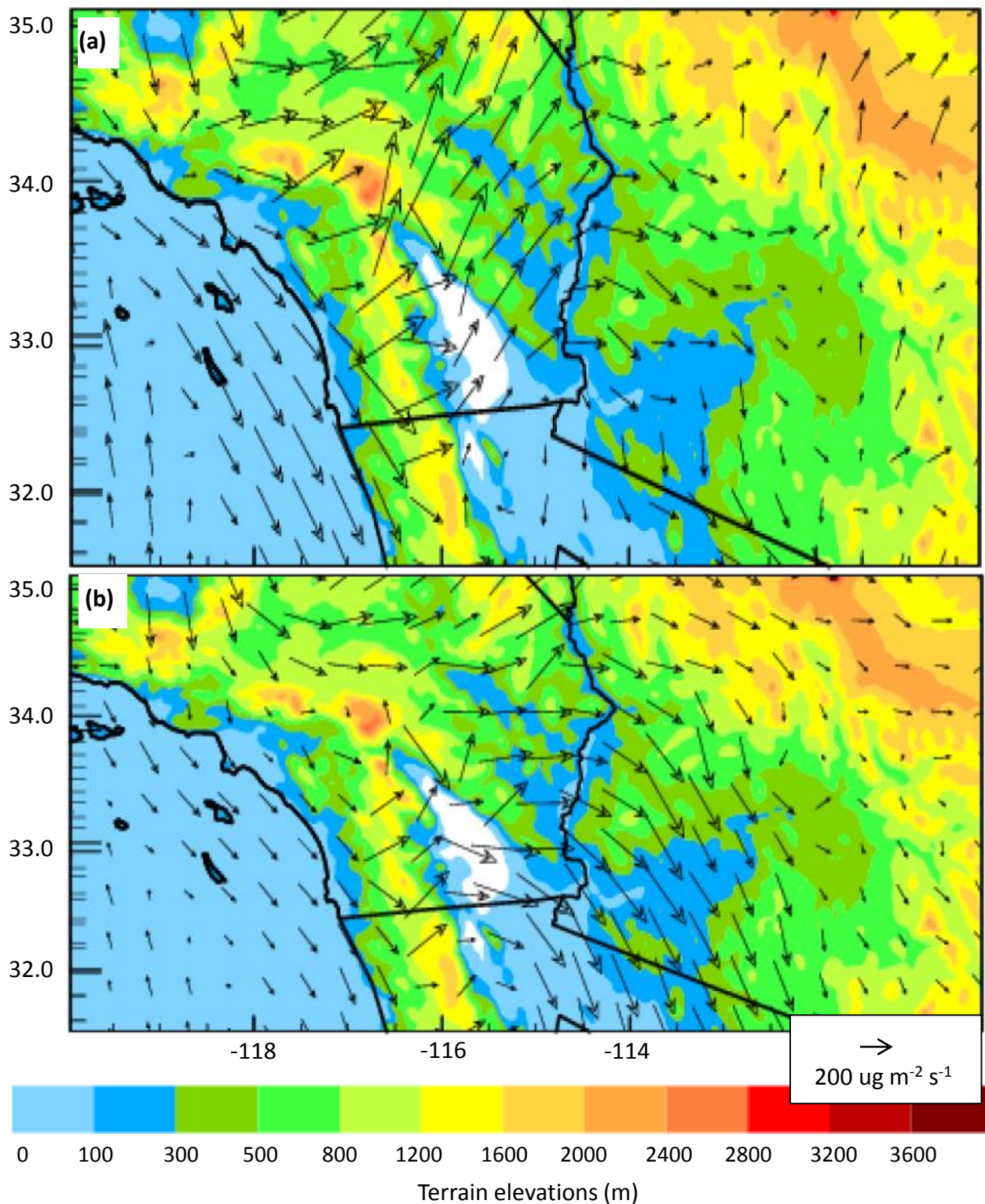


Figure S9: Integrated ozone transport flux differences (CTRL-noCA) from surface to 1400 m above ground-level: (a) average from 18Z to 02Z, July 16 to July 20, 2005, and (b) average from 03Z to 17Z, July 16 to July 20, 2005. Figures are based on 4 km resolution run. Comparing Figure S9 with 1 km run (Figure 12 in the manuscript), the Pass Channel Effect is much weaker at 4 km than that at 1 km both daytime and night time. In addition, the transport patterns are slightly different between 1km results and 4 km results.

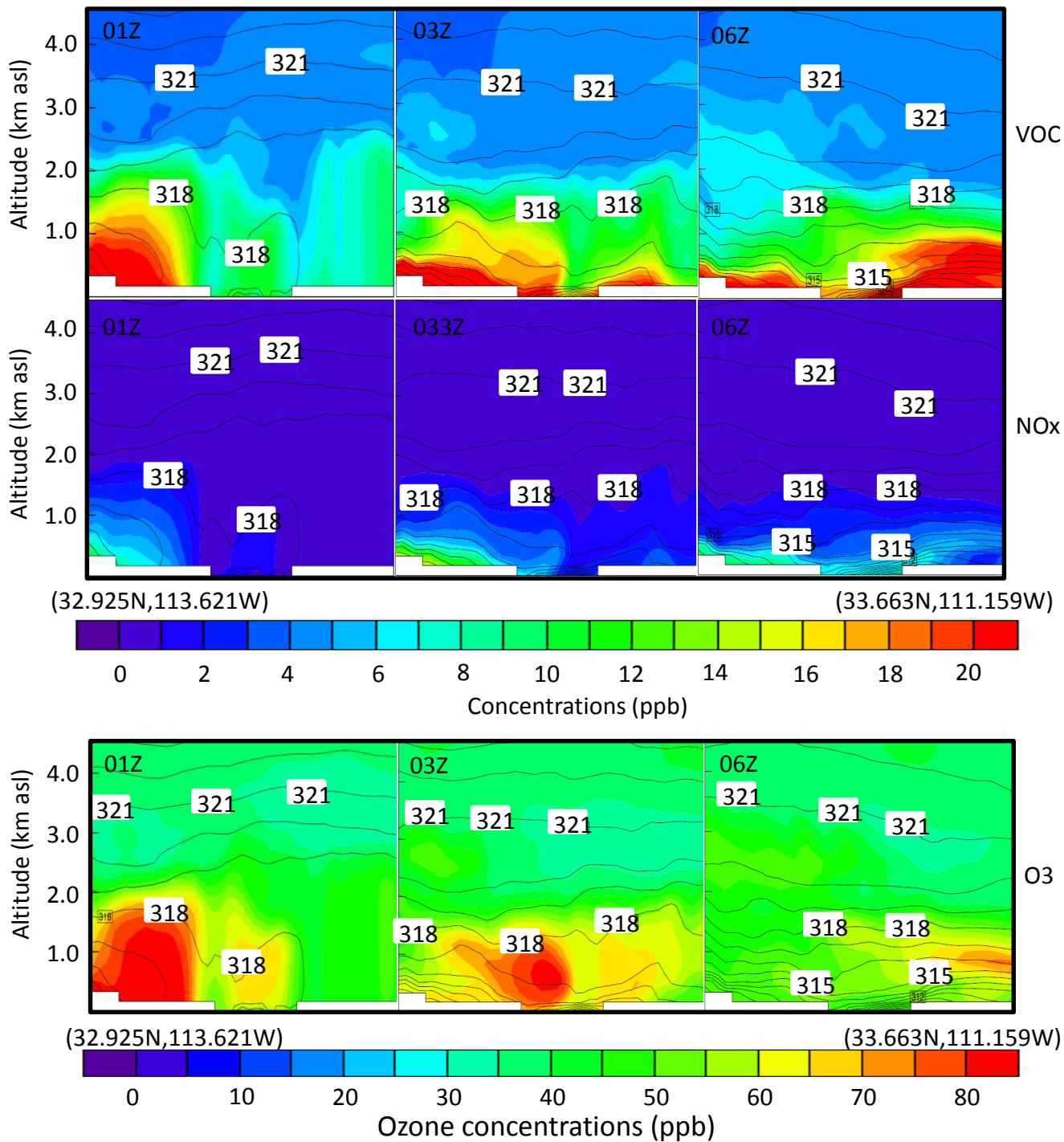


Figure S10: The vertical distribution of VOC (top), NO_x (middle), and O₃ (bottom) along the cross-section D'D (shown in Figure 1b) in Salton Sea Basin at 01Z, 03Z, and 06Z, July 18, 2005. Contours are potential temperature with 1-K interval. Data are from 4 km run. In comparing Figure S10 with 1 km run Figure (Figure 13 in the manuscript), the vertical distributions are over all similar but differences in detail at fine scales.

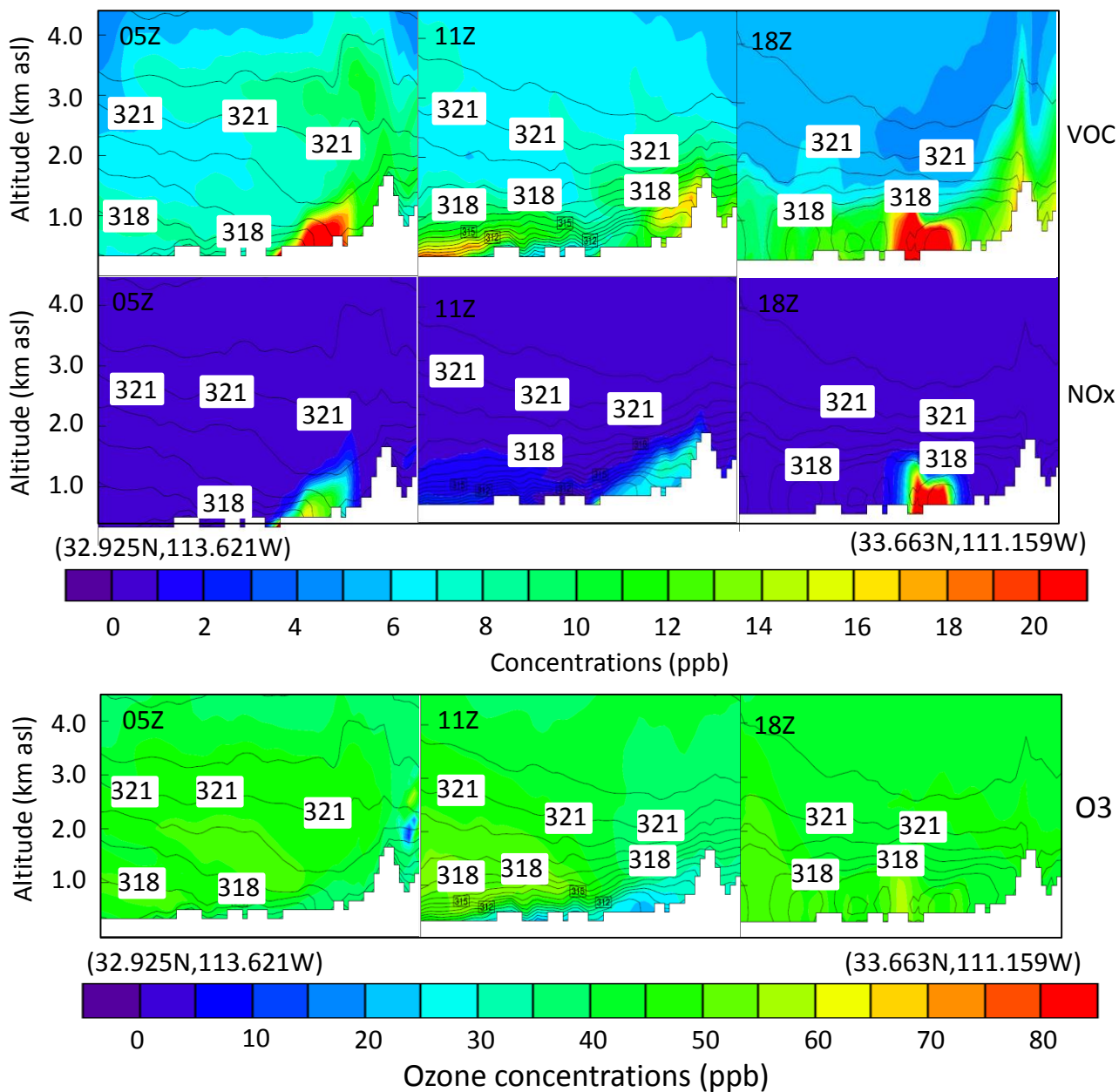


Figure S11: The vertical distribution of VOC (top), NO_x (middle), and O₃ (bottom) along the cross-section D'D (shown in Figure 1b) in Gila River Basin, Arizona at 05Z, 11Z, and 18Z, July 18, 2005. Contours are potential temperature with 1-K interval. Data are from 4 km resolution model run. In comparison Figure S11 with 1 km model run Figure (Figure 14 in manuscript), ozone concentration at 4 km resolution is much weak.